ORIGINAL ARTICLE

Additive manufacturing for capacitive liquid level sensors

Gianni Stano[1] · Attilio Di Nisio[2] · Anna Maria Lanzolla[2] · Mattia Alessandro Ragolia[2] · Gianluca Percoco[1]

Abstract

A new manufacturing wave concerning the Additive Manufacturing of sensors is spreading: several benefits, such as cost, time, and manual task reduction, can be achieved. The aim of the present research is the one-shot Additive Manufacturing of a low-cost capacitive sensor for liquid level sensing. The Material extrusion (MeX) technology was used to fabricate the proposed sensors (composed of a flexible substrate, two conductive electrodes, and a top flexible coverage), and a Design for Additive Manufacturing (DfAM) approach in conjunction with the 3D printing force analysis was performed. Very thin conductive tracks (0.5 mm) were manufactured to obtain a sensor having a final capacitance value of 125 pF, readable by common laboratory instrumentation. The sensor has been tested for the liquid level sensing using two different liquids, i.e., sunflower oil and distilled water, exhibiting very good sensitivity of 0.078 $\frac{pF}{mm}$ and 0.79 $\frac{pF}{mm}$, respectively, with high repeatability, thus obtaining sensing performances comparable with that of more expensive sensors found in literature. Moreover, the proposed sensor showed high linearity ($R^2 \geq 0.997$), which resulted in a maximum propagated level error of 1.4 mm. The present research proves that the inexpensive MeX technology can be successfully employed for the fabrication of high-performance capacitive sensors: the sensor manufacturing cost (related to raw materials) is 0.38 €, and no manual assembly tasks were performed. This study lays the foundation for the one-shot fabrication of smart structures with capacitive sensors on board, saving manufacturing time and cost.

Keywords Additive Manufacturing · 3D-printed sensors · Capacitive sensor · Liquid level sensing

1 Introduction

Additive Manufacturing Material extrusion (MeX) technology (in accordance with ISO/ASTM: 52,900: 2015) has been extensively used for the fabrication of smart structures, equipped with sensing systems [1]: in particular, MeX technology seems to be a valid alternative to the classic 2D sensor fabrication due to several features (i.e., inexpensive technology, multi-material manufacturing, geometric freedom) [2–4].

Several studies have been performed to reduce the gap of knowledge in the field of MeX-manufactured sensors: Arh et al. [5] proposed an experimental method to identify the dynamic piezo resistivity of unidirectionally printed structures providing coefficients needful for the building of analytical and numerical models; Cardenas et al. [6, 7] used high-intensity pulsed light to increase of two orders of magnitude the conductance of the tracks made up of commercial conductive filaments; Stano et al. [8], exploiting the Design of Experiment (DoE) approach, found out a relationship between process parameters (layer height and printing orientation) and electrical resistance (and variability) minimization; Maurel et al. [9] defined a novel framework to direct 3D print ion-lithium battery.

As outlined in [10], MeX technology is almost exclusively used to manufacture sensors based on the piezoresistive principle, ranging from classic applications such as static load detection [11, 12] up to dynamic load detection [13] which motivates Arh et al. [14] to develop a novel monolithic uniaxial accelerometer. Li et al. [15] developed a manufacturing procedure based on the MeX of commercial thermoplastic polyurethane (TPU) followed by an ultrasonic treatment to make the final structure conductive: they fabricated an auxetic sensor characterized by a Poisson ratio of –0.8 and a sensitivity of 2.661. A multilayered pressure

✉ Gianni Stano
  gianni.stano@poliba.it

1 Department of Mechanics, Mathematics and Management, Polytechnic of Bari, Via E. Orabona 4, 70125 Bari, Italy

2 Department of Electrical and Information Engineering, Polytechnic of Bari, Via E. Orabona 4, 70125 Bari, Italy

sensor has been fabricated using sacrificial material and conductive polylactic acid (PLA): the proposed sensor has been tested under different conditions proving its suitability for wearable applications [16].

Kim et al. [17] fabricated a smart structure composed of two sensors: a piezoresistive sensor for force detection and a temperature sensor. They attached the proposed device to gloves and shoes proving that MeX technology can be used for the fabrication of very low-cost sensors able to detect human motions. A not negligible aspect related to MeX-manufactured piezoresistive sensors regards the strong dependence between change in resistance and temperature [18]. Since the mechanism underlying this phenomenon in plastic materials doped with conductive fillers is not fully understood in literature and more research efforts are necessary to better characterize it, at the state of the art, the exploitation of these sensors to detect a change in temperature seems to be still not possible due to low repeatability [8, 18–21].

Recently, MeX technologies have been employed for the fabrication of capacitive-based sensors: Saari et al. [22] used the fiber encapsulation method to fabricate a capacitive force sensor having a sensitivity of $0.2 \frac{pF}{kN}$. Using a triple extruder MeX machine (support material, conductive material, insulator material), Liu et al. [23] developed a capacitive sensor for human blood pulse having a sensitivity of $1.9 \frac{pF}{N}$: in particular the total printing time was 35 min, while the support material dissolving time was almost 10 h. In 2021, Loh et al. [24] proposed a capacitive-based force sensor entirely manufactured through MeX technology: they connected the proposed sensor to a jamming universal gripper in order to obtain direct feedback (change in the row and column capacitance in the matrix) during the object manipulation (grasping, holding, and release).

As shown in [25], MeX technology can be successfully exploited for the fabrication of facemasks for radiation therapy: the usage of a multi-material 3D-printed setup can be the key enabler to fabricate embedded sensors into biomedical devices to obtain real-time feedback.

Several considerations have to be taken into account when AM multi-material extrusion technique is employed; the adhesion between the different extruded materials depends on several factors such as slicing parameters [26], interface geometries [27], material affinity [28], and inter-molecular diffusion [29]. The stretchable capacitive coplanar sensor is a class of capacitive sensor which is gaining a lot of interest in several application fields (i.e., sensing liquid level, humidity, temperature, motion detection). Generally, these sensors are fabricated by employing, at least, two different manufacturing technologies: one for the flexible dielectric substrate and one for the electrodes. At the state of the art, No-Additive Manufacturing (NAM) processes such as lithography, spin coating, and molding are employed for the substrate fabrication,

whereas AM technologies are often involved for the fabrication of the electrodes (on the other hand, the most widespread NAM technologies used for the fabrication of the electrodes are spray deposition, flexography, gravure, screen printing, etc. [30]). The AM processes exploited for the fabrication of the electrodes are generally inkjet (in all its variants) and Aerosol Jet micro-additive manufacturing: these approaches are expensive, and really often custom-made conductive materials (inks) are required due to a lack of them on the market [30–35].

In the present paper, the inexpensive MeX technology is used for the fabrication of a low-cost coplanar capacitive sensor: a Design for Additive Manufacturing (DfAM) approach has been used, and particular attention has been paid to the printing forces involved during the manufacturing process. In this way, really thin electrode tracks having a width of 0.5 mm and placed at a distance of 0.8 mm have been fabricated, thus overcoming the extrudability issues of the conductive thermoplastic material. In this way, a capacitance value of 125 pF has been obtained, which is readable by common measurement instrumentations. The sensor, consisting of (i) a dielectric flexible substrate, (ii) two electrodes, and (iii) a dielectric top cover, was fabricated in a single shot manufacturing step without recurring to further assembly tasks. The proposed sensors have been tested for liquid level sensing: a sensitivity of $0.078 \pm 0.002 \frac{pF}{mm}$ and $0.79 \pm 0.001 \frac{pF}{mm}$ was obtained for sunflower oil and water level detection, respectively. The main novelty of the present research is the one-shot fabrication of a flexible capacitive sensor characterized by high performance in terms of linearity, RMSE, and propagated error, pushing the boundaries of the inexpensive MeX technology for the manufacturing of smart structures with embedded capacitive sensors.

2 Materials and methods

At the state of the art, Material extrusion (MeX) technology has been unexploited for the fabrication of coplanar capacitive sensors due to the low manufacturability of conductive materials. In accordance with the coplanar capacitive sensor working mechanism (see Eq. (1) and Eq. (2)), the more the conductive tracks are thin and close to each other, the higher the final capacitance value is. The possibility to obtain high capacitance values readable by common measurement instrumentation is a key requirement for the fabrication of low-cost measurement circuits.

The main problem related to the additive manufacturing of thin conductive tracks has been addressed by (i) exploiting the Design for Additive Manufacturing (DfAM) approach and (ii) studying the forces involved during the manufacturing process to avoid the breakage of the brittle conductive material during the fabrication.

The main idea underlying the present work is shown in Fig. 1.

2.1 Design

The proposed capacitive sensor was designed to be used for liquid level sensing, and it was manufactured in a single shot 3D printing cycle: it consists of (i) a flexible substrate of thermoplastic polyurethane (TPU), (ii) two coplanar electrodes made up of conductive polylactic acid (CPLA), and (iii) a top cover made up of TPU which seals off the electrodes, thus avoiding the direct contact of the electrodes with the liquid during the sensing. After the manufacturing process, the sensor covered with a top layer of TPU (henceforth called TPU-covered) is ready to be used for liquid level sensing.

The overall sensor dimensions are shown in Fig. 2a: in particular, the substrate is 171 mm long and 55 mm wide, while its thickness is 0.4 mm; the top TPU cover (Fig. 2b) is 0.3 mm thick.

The design of the electrodes is a crucial point to obtain a measurable capacitance value: on one hand, thin conductive tracks really close to each other are required to obtain readable capacitance values; on the other hand, technological constraints must be taken into account when conductive filaments are extruded. In accordance with [31], the capacitance of coplanar capacitive sensors is defined by the following equation:
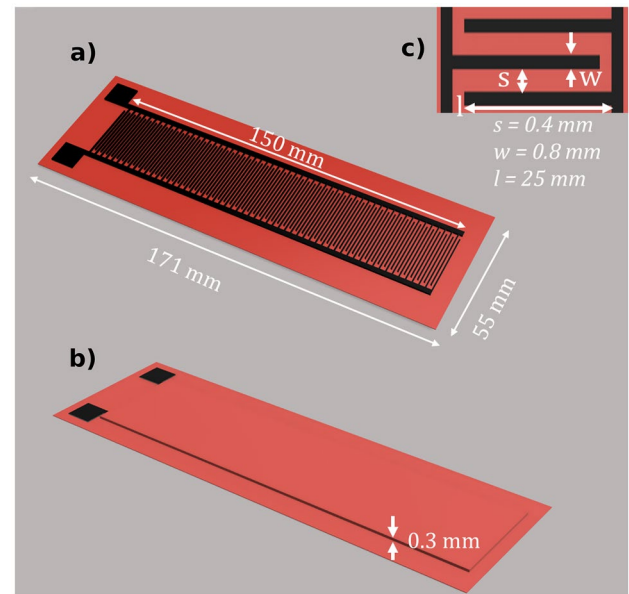

Fig. 2 Design of the coplanar capacitive sensor, in red the flexible substrate and in black the two electrodes: **a** uncovered sensor, **b** TPU-covered sensor, and **c** design variables

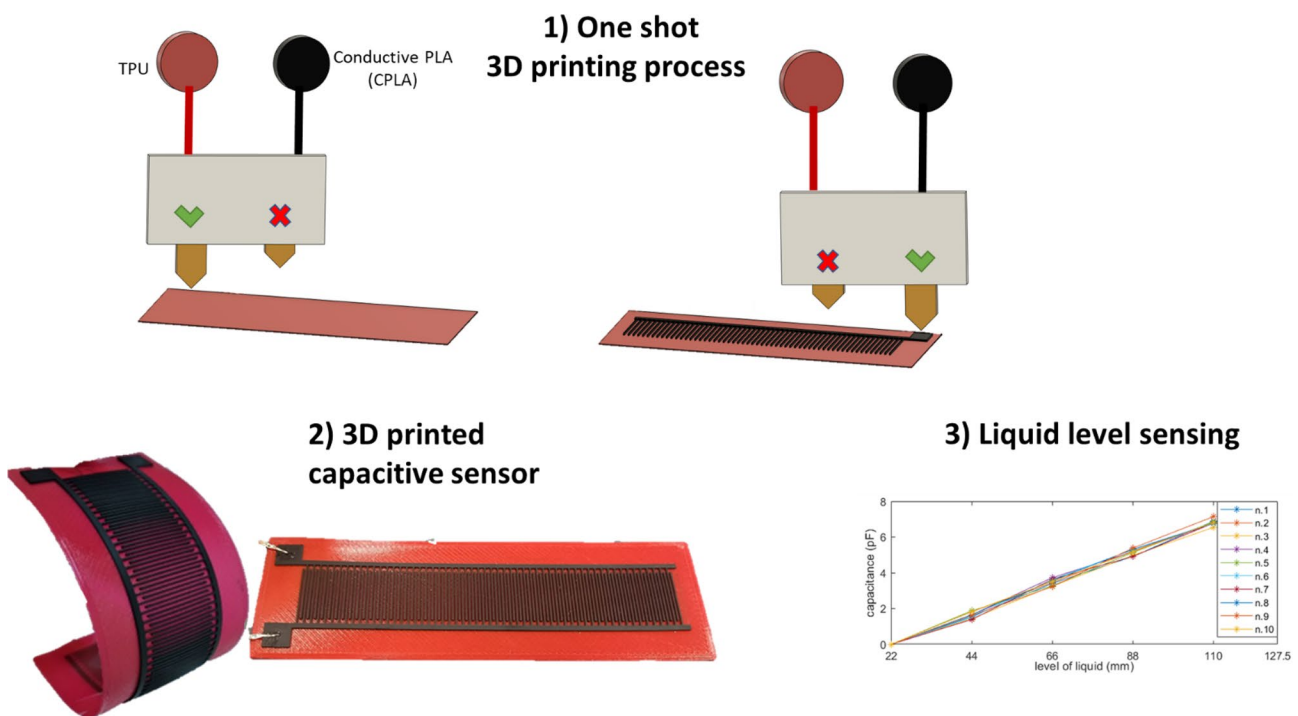$$C = Nl\varepsilon_0\varepsilon_{ea}\frac{K(\sqrt{1-k_0^2})}{K(k_0)} \tag{1}$$

Fig. 1 Workflow underlying the present research

where C (pF) is the capacitance of the whole sensor, N (dimensionless) is the number of electrodes pairs, l (mm) is the length of each electrode along x-axis, ε_0 is the vacuum dielectric constant ($\frac{pF}{mm}$), ε_{ea} (dimensionless) is the effective dielectric constant of capacitive sensor in the air (further details about this parameter are well explained in [31]), and $K(k_0)$ (dimensionless) is the elliptical integral of the first kind in terms of k_0, where k_0 is defined as follows

$$k_0 = \frac{s}{s + 2w} \tag{2}$$

where s (mm) and w (mm) are the electrode spacing and width, respectively. Thus, the only design parameters that can be set in order to maximize the final capacitance are N, l, s, and w (see Fig. 2c).

As a matter of fact, the free design variables are the l parameter (length of the single electrode, as shown in Fig. 2c) and the overall electrodes length (see Fig. 2a), which have been arbitrarily set as 25 mm and 150 mm, respectively. Consequently, considering all the manufacturing constraints (detailed in Sect. 2.2), it was found the best N, s, and w values to maximize the final capacitance to be 57, 0.8 mm and 0.5 mm, respectively, thus obtaining a predicted capacitance of 82.7 pF from Eq. (1).

The DfAM approach was used to successfully set w: considering the printing orientation (sensor flat on the build plate with the flexible substrate in contact with it), the w parameter depends on the line width process parameters, which in turn must be equal to the nozzle diameter. From Eq. (1), the need to minimize w stands out: the following requirement is in contrast with conductive material processability (the bigger the nozzle, the less are the printing issues such as filament breakdown and coggled nozzle). By setting further process parameters (detailed in Sect. 2.2), it has been possible to use a 0.5-mm nozzle and set $w = 0.5$ mm: it means that every conductive track will be the result of one single extruded line. Similar considerations can be drawn for the s parameter: using a trial-and-error approach, it was found that the minimum spacing between two adjacent conductive tracks allowed by the fused filament fabrication (FFF) machine was 0.8 mm. By setting lower values, an overlapping between adjacent conductive tracks occurred, due to the filament expansion after the extrusion: in this way, no capacitance values were measured, but only resistance

ones. The electrode thickness was arbitrarily set as 0.8 mm; however, lower values are allowed. Moreover, the sensor was equipped with two square pads (side equal to 10 mm) to weld electrical wires for the connection with the measurement instrumentation.

2.2 Additive Manufacturing

The sensor has been fabricated in a monolithic way, exploiting several advantages of the FFF technology, such as the possibility to extrude more materials at the same time and the reduction of assembly tasks [36, 37]. A multi-material extrusion 3D printer (Ultimaker 3, Ultimaker, Netherland) and two commercial materials were used (see Table 1). An overview of the multi-material extrusion process is shown in Fig. 1. For TPU and CPLA, 0.8- mm and 0.5-mm nozzles were used, respectively.

As a matter of fact, the smaller the nozzle size is, the more the level of detail is when conductive materials (generally PLA-based doped with CNTs) are used: the general advice provided by filament suppliers regards the usage of nozzles having a diameter equal to 0.6–0.8 mm. The main problem which could occur when nozzles smaller than 0.6 mm are employed is the filament breakdown between the gears pushing it into the extruder: the doping elements (i.e., CNTs) scattered into the plastic matrix make the filament very brittle.

To overcome this issue, it becomes crucial to set the right process parameters to reduce the printing force (F_p): in this way, the force between the gears and the raw filament (F_{gf}), which is responsible for the filament breakage, will be reduced as well, thus avoiding the filament breakage. Indeed, F_{gf} must be higher than F_p: in this way, the gears will push the raw filament into the extruder.

$$F_{gf} \geq F_p \tag{3}$$

In Fig. 3, a simplified model of the forces occurring during the manufacturing process is provided (the friction among the raw filament and the Teflon guiding tube has been neglected).

In accordance with [38], F_p can be calculated as the contribution of two forces:

$$F_p = F_n + F_{dep} \tag{4}$$

Table 1 Materials used for sensor manufacturing

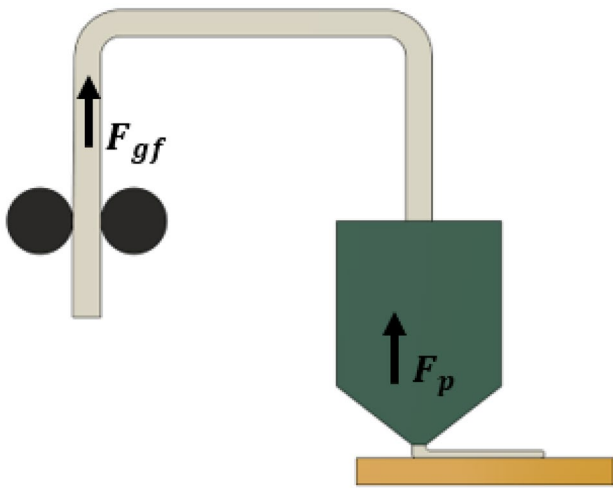| Material	Name	Properties	Manufacture	Sensor parts
Thermoplastic polyurethane	TPU	• Shore A hardness equal to 95 • Elongation at break equal to 580%	Ultimaker (Netherland)	• Flexible substrate • Top cover
Conductive polylactic acid	CPLA	• Resistivity of 15 $\Omega \cdot$ cm along the layers • Resistivity of 20 $\Omega \cdot$ cm perpendicular to the layers	FiloAlfa (Italy)	• Electrodes • Pads

Fig. 3 Simplified FFF force model

where F_n is the "nozzle force" (Eq. (5)), and it refers to the melting process taking place inside the extruder (the extruder can be divided into 3 different regions: in each one, a pressure increment occurs), while F_{dep} is the "deposition force" referring to the interaction between just extruded filament and build plate (or previously extruded filament) taking into account the counterpressure related to melting filament downstream of the nozzle: this force has been introduced by Percoco et al. [38] in 2021, and it links process parameters of the extruded filament with the classic F_n, well known in scientific literature [39]:

$$F_n = (\Delta P_1 + \Delta P_2 + \Delta P_3)A_f \tag{5}$$

where ΔP_1, ΔP_2, and ΔP_3 are the pressure increment into the three extruder regions, while A_f is the cross-section of the filament. To better understand each term included into F_n and F_p and how they affect the total printing force F_p, the reader is addressed to [38, 40].

The nozzle geometry of this work is the same as [38] (Ultimaker nozzle), while rheological parameters for CPLA are not available in scientific literature, and classic PLA ones have been used.

It has been pointed out that to reduce F_p, two parameters need to be set: printing temperature and layer height; when they increase, the total printing force decreases (see Eq. (6)).

$$F_p = f^{-1}(layer\ height,\ printing\ temperature) \tag{6}$$

It appears clear that the only way to manufacture thin conductive tracks (and reduce the total printing force) is to maximize the layer height and the printing temperature. Hence, the exploitation of the 0.5 mm nozzle for the brittle CPLA conductive filament is allowed by setting (i) the layer height (*lh*) parameter equal to 0.2 mm, unlike for the classic

Table 2 Process parameters

	TPU	CPLA
Nozzle size (mm)	0.8	0.4
Layer height (mm)	0.2	0.2
Printing temperature (°C)	223	225
Line width (mm)	0.8	0.5
Printing speed (mm/s)	30	25
Flow (%)	106	110

MeX scenario where high details are reached by setting a low layer height value (i.e. 0.05 mm) [41], and (ii) the printing temperature (T_p) equal to 230 °C, higher than the suggested printing temperature range of 190–210 °C provided by the supplier.

A 2^3-factorial plan (three repetitions) was conducted to set the best *lh* and T_p values: the number of printing successes for every combination (no filament breakdown and no nozzle clogging) extruding CPLA was measured. Three values of *lh* (0.1, 0.2, and 0.3 mm) and T_p (190, 210, and 230 °C) were studied, and the best combination resulting in the maximization of the printing success was found to be *lh* equal to 0.2 mm and T_p equal to 230 °C. In this way, thin conductive tracks with a width (parameter in Sect. 2.1) of 0.5 mm were fabricated without any filament breakdown despite a huge number (more than 20) of consecutive printed sensors.

In Table 2, the main process parameters set for both materials are summarized.

The total cost of raw materials for the TPU-covered sensor, estimated by the slicer software (Ultimaker Cura 4.6), was 0.38 €, while the manufacturing time was 41 min. Figure 4a, b show, respectively, the developed sensor during the 3D printing process and the sensor flexibility (potentially, it can be easily attached to irregular and non-conventional structures, paving the way for its exploitation in the field of wearable sensors).

The main advantage of the TPU-covered sensor, from a manufacturing standpoint, is the total absence of post-processing to seal off the electrodes: very often manual tasks, i.e., coating, strongly related to the operators' skills are employed [42, 43]. In Fig. 4c, the TPU-covered sensor and an uncovered version (i.e., the same sensor without the top TPU cover) are shown.

Finally, to prove the additive manufacture method robustness, 10 samples of each version (see Fig. 3c) have been printed, carrying out the following conclusions: (i) no filament breakdown occurred, and (ii) the TPU-covered mean capacitance value was 125.5 pF with a very low standard deviation of 0.7 pF, due to a not uniform electrical resistance of the raw conductive filaments (before of being melted into the nozzle) and noise effects occurring during the printing such as vibrations and room conditions.
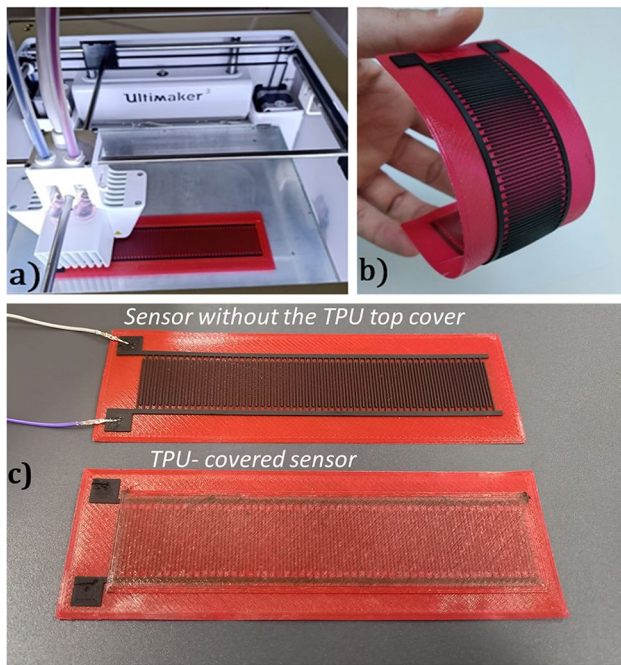
Fig. 4 **a** Additive Manufacturing of the proposed sensor, **b** sensor flexibility, and **c** the proposed TPU-covered sensor and its uncovered version (no top TPU cover)

2.3 Measurement setup and protocol

The measurement setup consists of the following (Fig. 5):

(i)   A custom-made 3D-printed tank, which presents a vertical channel in which it was manually injected a constant quantity of liquid by means of a syringe. The vertical channel avoids the spatter of liquid droplets on the surface of the sensors, which could lead to errors in the liquid level measurement.
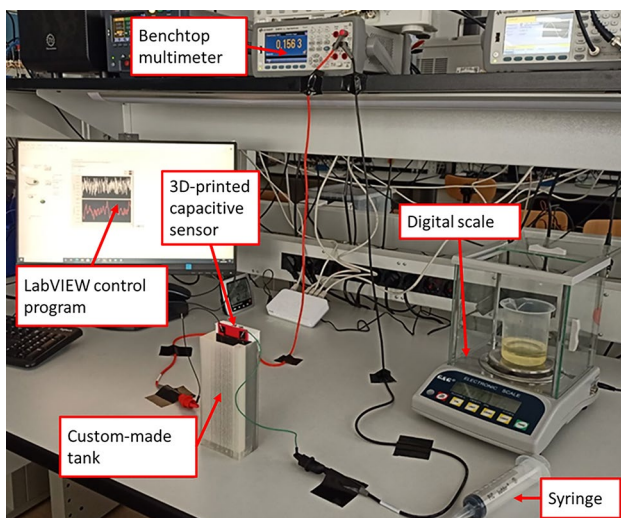
(ii)   A 34461A digital multimeter (Keysight Technologies, Santa Rosa, CA, USA), with 6 ½ digits of resolution, for accurate measurements of capacitance in a range of 1 nF.

(iii)   A control program developed in LabVIEW® by National Instruments Corp., to easily manage the system, providing real-time monitoring and data storage for further processing.

(iv)   A digital scale with a resolution of 0.001 g to measure the amount of liquid to inject.

Before performing the experiments, a preliminary test was performed to prove the tightness of the TPU cover when immersed in two different liquids. The TPU-covered sensor was kept in a tank full of water for 48 h, and no cover degradation was observed. Afterwards, the same test was performed using sunflower oil, and no difference was observed.

The TPU-covered was first tested for the sensing of sunflower oil level and then for distilled water level: several conclusions can be drawn, proving that its behavior is consistent with capacitive sensors described in the literature.

The following measurement protocol was used for both the liquids: the same amount of liquid, weighed by means of the high-accuracy digital scale, was injected for a total of 5 steps; at each step, a settling time of 30 s was waited from the injection of the liquid, and the average of 20 consecutive capacitance readings was computed, in order to reduce noise. The results of test number one for the sunflower oil are shown in Fig. 6. The whole procedure has been repeated 10 times (a total of 10 test cycles) to assess the repeatability. After each cycle, a time of 4 min was waited, in order to manually dry the sensor and empty the tank. All tests have been performed after zeroing the offset capacitance of the multimeter and leads.
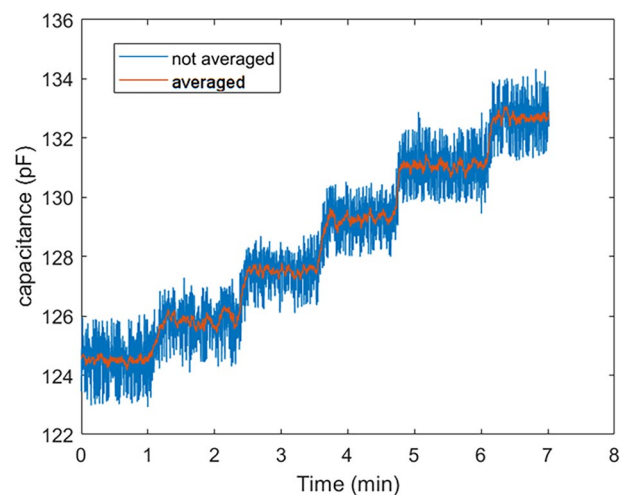

Fig. 5 Measurement setup

Fig. 6 Capacitance of the TPU-covered sensor vs time. Test 1 with sunflower oil

3 Results and discussion

In this section, the TPU-covered sensor was tested for liquid level sensing. Two different liquids were used to test the sensor, i.e., distilled water and sunflower oil, and different metrological characteristics were evaluated (i.e., sensitivity, linearity, offset, and repeatability).

Moreover, the temperature was measured during the performed tests (since it affects sensor capacitance), and it was assessed to be stable (about 20 °C). A detailed analysis of the effect of temperature on the capacitance of the proposed capacitive sensors was carried out in [44], highlighting a nonlinear dependence of capacitance on temperature and obtaining a model to compensate for its effect. Using the testing setup and protocol detailed in Sect. 2.3, the results described in the following section have been obtained.

Figure 7a, b show the results of the performed tests for the TPU-covered sensor: in particular, the offset of each curve was reduced to zero to provide a better comparison. The offsets of each curve with respect to the 1st one are separately shown in Fig. 8, for water and sunflower oil. Table 3 lists the main metrological parameters obtained by analyzing data presented in Figs. 7 and 8 and reports a comparison with Paczesny et al. [32], where ink-jet printing technology was employed to fabricate capacitive level sensors. Moreover, comments about the key aspects of each kind of sensor are provided.

Very high linearity of the sensitivity to the level of both liquids has been obtained, comparable to other high linearity capacitive level sensors found in the literature [31, 32,

Fig. 7 Capacitance vs level of liquid: **a** TPU-covered in sunflower oil, **b** TPU-covered in distilled water, **c** tape-covered in distilled water
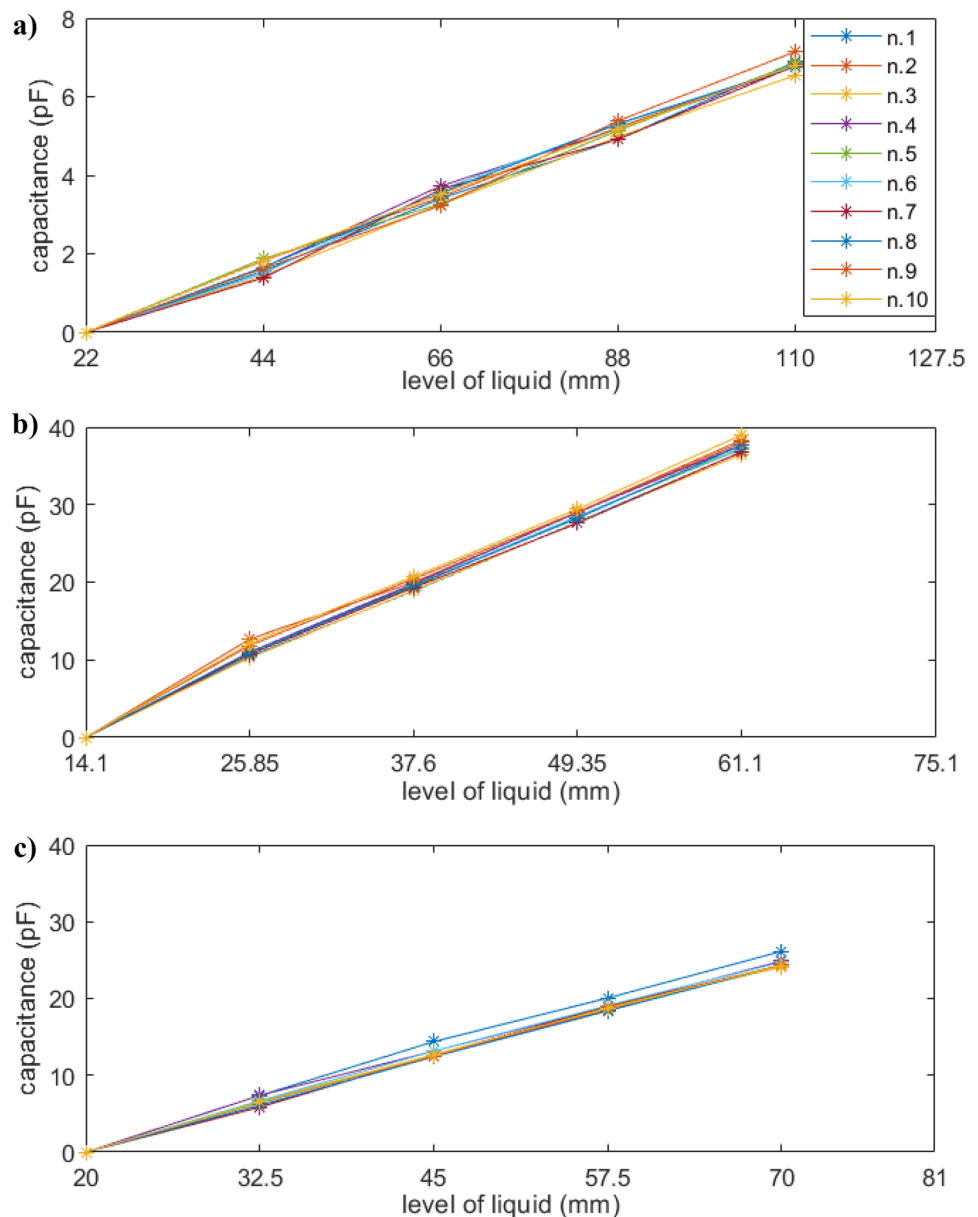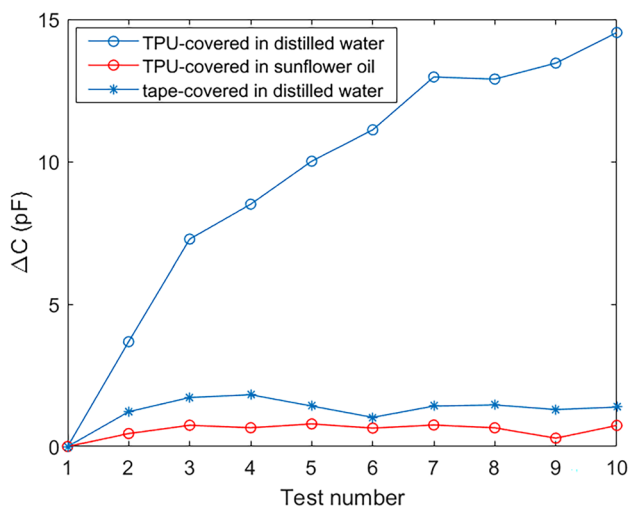
Fig. 8 Offset of linear regression curves with respect to the 1st one

43], with R^2 coefficient higher than 0.9973 and a root-mean-square error (RMSE) lower than 1.7% of the full-scale output (FSO, calculated as the difference between the maximum and minimum of the moving averaged capacitance for each test). Linearity has been reported as percentage of the FSO, in order to compare between different sensitivities. As shown in Table 3, a maximum propagated error of 1.4 mm is obtained by dividing the nonlinearity error (RMSE) by the sensitivity of the sensor, thus ensuring the good linearity performances of the proposed sensors.

The sensitivity of the sensor to oil and water is obtained by performing a linear regression on each curve and by averaging the results of the 10 performed tests presented in Fig. 7a, b. As expected, the sensitivity to sunflower oil is one order of magnitude lower than the one obtained with distilled water (0.078 $\frac{pF}{mm}$ versus 0.79 $\frac{pF}{mm}$, as reported in Table 3), since sunflower oil is characterized by different electrical properties (i.e., lower electrical conductivity and dielectric constant).

As shown in Fig. 8, when sensing sunflower oil level, the offsets with respect to the 1st test shows a random distribution with a mean and standard deviation of 0.64 ± 0.16 pF (Table 3). In the authors' opinion, this random offset could be due to (i) changes in room conditions (i.e., slight temperature change) [8], (ii) changes in tank conditions (after each test cycle the tank was manually cleaned up, and some drops could have remained into the tank), and (iii) slight changes in the position of connection wires [45, 46].

When sensing water level, instead, the sensor presents an increasing offset for each test, spanning a range up to 14.5 pF, as shown in Fig. 7a: compared to oil sensing, the offset is meaningfully high (806%), and it is not randomly distributed, but it is increasing. Indeed, in addition to the random variable changes, above described, in this case, another important phenomenon takes place: the TPU material, of which the top cover is made up, is characterized by a water absorption value of 0.18% in accordance with the ASTM D570 test method (material data sheet). As a matter of fact, after each test cycle, a certain amount of water gets trapped into the TPU cover leading to an ever-increasing initial capacitance value (initial offset) from test cycle n to $n+1$, with $n=1, \ldots, 9$. Instead, during oil sensing, the sensor does not show increasing offset, since the employed TPU material does not provide any evidence of oil absorption, unlike for water. Nevertheless, despite the increasing initial offset, the TPU-covered version can be employed in short-term tests by performing a zeroing procedure to compensate the offset, since the effect of water absorption seems to not affect sensing performances in the short period. The next studies will focus on the TPU-covered sensor lifespan.

However, in order to provide reliable measurements for long-duration tests, in this paper, a "tape-covered" version of the capacitive sensor is proposed where the conductive electrodes of the 3D-printed sensor have been sealed off with adhesive tape in order to keep them isolated from the surrounding environment. The sealing process represents a further manual task; nevertheless, it results easy to be performed and inexpensive: the authors present this solution as a good alternative to the TPU-covered sensor

Table 3 Metrological characteristics of the proposed sensors. Results are expressed as mean or mean $\pm$ std. Propagated error is obtained by dividing the linearity error (RMSE) by the sensitivity of the sensor

Liquid	Sensor	Sensitivity ($\frac{pF}{mm}$)	Linearity				Offset (pF)	FSO (pF)	Comments
			R^2	RMSE		Propagated error (mm)			
				(pF)	(% FSO)				
Oil	**TPU-covered**	0.078 ± 0.002	0.9977	0.109	1.6	1.4	0.64 ± 0.16	6.8	No zeroing procedure required
Water	**TPU-covered**	0.79 ± 0.01	0.9973	0.656	1.7	0.8	---	37.5	Zeroing procedure required
	Tape-covered	0.49 ± 0.01	0.9988	0.281	1.1	0.6	1.42 ± 0.24	24.6	No zeroing procedure required
	Literature [32]	0.074	0.998	---	---	---	---	---	More expensive manufacturing technology; multiple manufacturing steps

for a long-period sensor usage in water, thus overcoming the water absorption problem of the TPU cover. As for the TPU-covered sensor, also the tape-covered sensor was kept in a tank full of water for 48 h, and no cover detachment was observed. It should be said that a little amount of water is sufficient to short circuit the electrodes, thus preventing capacitance measurements; hence, the 48-h test was necessary to assess the tightness of the adhesive tape.

The same measurement protocol was applied to the tape-covered sensor, and the results are shown in Fig. 6c, and the main metrological parameters are summarized in Table 3.

As for the TPU-covered sensor, high linearity is observed for the tape-covered sensor, with a R^2 coefficient of 0.9988 and a RMSE of 1.1% of the FSO. The TPU-covered sensor presents a sensitivity of 0.49 $\frac{pF}{mm}$, which is about 60% higher than the TPU-covered sensor: as well explained in [31], the top cover of the sensor is accountable for the different sensitivity; in fact, the main differences between the two top covers (embedded TPU cover and adhesive tape cover, respectively) are (i) the cover thickness and (ii) the dielectric constant of the cover material.

The obtained results are really appealing: for example, if compared to [32], the proposed TPU-covered and tape-covered sensors present a sensitivity to water level one order of magnitude higher, with the advantage that they are manufactured in a monolithic way and by using a much cheaper fabrication technology. Moreover, the proposed sensors can be directly integrated into smart structures in the same fabrication, whereas ink-jet printing technology [32] requires further assembly tasks, as well as manual procedures to isolate the electrodes from the liquid.

Finally, the tape-covered sensor presents a very low offset (1.42 ± 0.24 pF, as shown in Table 3) of the same order of magnitude as the offset observed for the TPU-covered sensor when the oil was employed: as previously described, the offset is due to slight changes in room, tank, and wire conditions.

To summarize, the assembly-free TPU-covered version can be employed for oil level sensing (without restrictions) and water level sensing (by applying a zeroing procedure), while the tape-covered version can be employed for water sensing without applying any zeroing procedure.

4 Conclusion

In the present paper, the Material extrusion (MeX) Additive Manufacturing (AM) technology has been employed for the fabrication of a coplanar capacitive sensor for liquid level sensing.

The Design for Additive Manufacturing (DfAM) approach, in conjunction with the printing forces analysis,

has been exploited to fabricate a total of 57 conductive electrode tracks having a width of 0.5 mm and a spacing of 0.8 mm between them. In this way, a readable capacitance value of 125 pF was achieved (measurable from common measurement instrumentations). The main benefit of the proposed manufacturing approach consists of the one-shot fabrication of the whole sensor (flexible TPU substrate, conductive electrodes, and top TPU cover): no assembly tasks were employed, resulting in material cost and time saving (0.38 € and 40 min, respectively).

The proposed low-cost sensor has been tested for liquid level sensing: a very good sensitivity of 0.078 $\frac{pF}{mm}$ ($R^2 = 0.9977$) and 0.79 $\frac{pF}{mm}$ ($R^2 = 0.9973$) was achieved for sunflower oil and distilled water level, respectively, proving that the performances of the proposed low-cost sensor are comparable with that of more expensive sensors found in the literature. The sensor presented very high linearity, with a propagated nonlinearity error lower than 1.4 mm.

The present work aims at pushing the role of the inexpensive MeX technology for the fabrication of capacitive sensors embedded into 3D-printed structures: non-conventional tanks as well as soft structures actuated by means of fluids (fluidic actuators) can be 3D printed in the same fabrication cycle alongside with the proposed capacitive sensor for liquid level detection, resulting in fabrication time and cost saving.

Declarations

References

1. Kalkal A et al (2021) Recent advances in 3D printing technologies for wearable (bio)sensors. Addit Manuf 46(June):102088. https://doi.org/10.1016/j.addma.2021.102088

2. M. Schouten, G. Wolterink, A. Dijkshoorn, D. Kosmas, S. Stramigioli and G. Krijnen (2021) "A Review of Extrusion-Based 3D Printing for the Fabrication of Electro- and Biomechanical Sensors," in IEEE Sensors Journal 21(11):12900–12912. https://doi.org/10.1109/JSEN.2020.3042436

3. Khosravani MR, Reinicke T (2020) 3D-printed sensors: current progress and future challenges. Sens Actuators A Phys 305:111916. https://doi.org/10.1016/j.sna.2020.111916

4. Bekas DG, Hou Y, Liu Y, Panesar A (2019) 3D printing to enable multifunctionality in polymer-based composites: a review. Compos Part B Eng 179(October):107540,. https://doi.org/10.1016/j.compositesb.2019.107540

5. Arh M, Slavič J, Boltežar M (2020) Experimental identification of the dynamic piezoresistivity of fused-filament-fabricated structures. Addit Manuf 36(April):101493. https://doi.org/10.1016/j.addma.2020.101493

6. Cardenas JA et al (2020) Flash ablation metallization of conductive thermoplastics. Addit Manuf 36(March):101493. https://doi.org/10.1016/j.addma.2020.101409

7. Lazarus N, Tyler JB, Cardenas JA, Hanrahan B, Tsang H, Bedair SS (2022) Direct electroless plating of conductive thermoplastics for selective metallization of 3D printed parts. Addit Manuf 55(March):1027930. https://doi.org/10.1016/j.addma.2022.102793

8. Stano G, Nisio D, Lanzolla AM et al (2020) Fused filament fabrication of commercial conductive filaments : experimental study on the process parameters aimed at the minimization, repeatability and thermal characterization of electrical resistance. Int J Adv Manuf Technol 111:2971–2986

9. Maurel A et al (2020) Considering lithium-ion battery 3D-printing via thermoplastic material extrusion and polymer powder bed fusion. Addit Manuf 37(July):2021. https://doi.org/10.1016/j.addma.2020.101651

10. H. Liu et al (2021) "3D Printed Flexible Strain Sensors: From Printing to Devices and Signals," Advanced Materials 33(8):2004782. https://doi.org/10.1002/adma.202004782

11. Watschke H, Goutier M, Heubach J, Vietor T, Leichsenring K, Böl M (2020) "Novel Resistive Sensor Design Utilizing the Geometric Freedom of Additive Manufacturing," Applied Sciences 11(1):113. https://doi.org/10.3390/app11010113

12. Kim K, Park J, Suh J, Kim M, Jeong Y, Park I (2017) Sensors and actuators a : physical 3D printing of multiaxial force sensors using carbon nanotube (CNT)/thermoplastic polyurethane (TPU) filaments. Sens Actuators A Phys 263:493–500. https://doi.org/10.1016/j.sna.2017.07.020

13. Maurizi M et al (2019) Dynamic measurements using FDM 3D-printed embedded strain sensors. Sensors (Switzerland) 19(12):1–15. https://doi.org/10.3390/s19122661

14. M. Arh, J. Slavič, and M. Boltežar (2020) "Design principles for a single-process 3d-printed accelerometer – theory and experiment," Mechanical Systems and Signal Processing vol. 152, p. 107475, https://doi.org/10.1016/j.ymssp.2020.107475

15. Li B, Liang W, Zhang L, Ren F, Xuan F (2022) TPU/CNTs flexible strain sensor with auxetic structure via a novel hybrid

16. Alsharari M, Chen B, Shu W (2022) Sacrificial 3D printing of highly porous, soft pressure sensors. Adv Electron Mater 8(1):1–12. https://doi.org/10.1002/aelm.202100597

17. Kim HG, Hajra S, Oh D, Kim N, Kim HJ (2021) Additive manufacturing of high-performance carbon-composites: an integrated multi-axis pressure and temperature monitoring sensor. Compos Part B Eng 222(April):109079. https://doi.org/10.1016/j.compositesb.2021.109079

18. Lanzolla AML, Attivissimo F, Percoco G, Ragolia MA, Stano G, Di Nisio A (2022) Additive manufacturing for sensors: piezoresistive strain gauge with temperature compensation. Appl Sci 12(17). https://doi.org/10.3390/app12178607

19. Mohiuddin M, Hoa SV (2011) Temperature dependent electrical conductivity of CNT-PEEK composites. Compos Sci Technol 72(1):21–27. https://doi.org/10.1016/j.compscitech.2011.08.018

20. Kwok SW et al (2017) Electrically conductive filament for 3D-printed circuits and sensors. Appl Mater Today 9:167–175. https://doi.org/10.1016/j.apmt.2017.07.001

21. Daniel F, Patoary NH, Moore AL, Weiss L, Radadia AD (2018) Temperature-dependent electrical resistance of conductive polylactic acid filament for fused deposition modeling. Int J Adv Manuf Technol 99(5–8):1215–1224. https://doi.org/10.1007/s00170-018-2490-z

22. Saari M, Xia B, Cox B, Krueger PS, Cohen AL, Richer E (2016) Fabrication and analysis of a composite 3D printed capacitive force sensor. 3D Print Addit Manuf 3(3):137–141. https://doi.org/10.1089/3dp.2016.0021

23. Liu GD, Wang CH, Jia ZL, Wang KX (2021) An integrative 3D printing method for rapid additive manufacturing of a capacitive force sensor. J Micromech Microeng 31(6). https://doi.org/10.1088/1361-6439/abf843

24. Loh LYW, Gupta U, Wang Y, Foo CC, Zhu J, Lu WF (2021) 3D printed metamaterial capacitive sensing array for universal jamming gripper and human joint wearables. Adv Eng Mater 2001082:1–9. https://doi.org/10.1002/adem.202001082

25. Asfia A, Novak JI, Rolfe B, Kron T (2022) Development of a patient-specific immobilisation facemask for radiation therapy using additive manufacturing, pressure sensors and topology optimisation. Rapid Prototyp J 28(5):945–952. https://doi.org/10.1108/RPJ-09-2021-0241

26. Tamburrino F, Graziosi S, Bordegoni M (2019) The influence of slicing parameters on the multi-material adhesion mechanisms of FDM printed parts: an exploratory study. Virtual Phys Prototyp. https://doi.org/10.1080/17452759.2019.1607758

27. Ribeiro M, Carneiro OS, da Silva AF (2019) Interface geometries in 3D multi-material prints by fused filament fabrication. Rapid Prototyp J 25(1):38–46. https://doi.org/10.1108/RPJ-05-2017-0107

28. Lopes LR, Silva AF, Carneiro OS (2018) Multi-material 3D printing: the relevance of materials affinity on the boundary interface performance. Addit Manuf 23(March):45–52. https://doi.org/10.1016/j.addma.2018.06.027

29. Yin J, Lu C, Fu J, Huang Y, Zheng Y (2018) Interfacial bonding during multi-material fused deposition modeling (FDM) process due to inter-molecular diffusion. Mater Des 150:104–112. https://doi.org/10.1016/j.matdes.2018.04.029

30. Rivadeneyra A, López-Villanueva JA (2020) Recent advances in printed capacitive sensors. Micromachines

31. Yang Q et al (2017) Inkjet-printed capacitive sensor for water level or quality monitoring theoretically and experimentally. Mater Chem A. https://doi.org/10.1039/C7TA05094A

32. Paczesny D, Tarapata G, Michał M, Jachowicz R (2015) "The Capacitive Sensor for Liquid Level Measurement Made with Ink-jet Printing Technology," Procedia Engineering, vol. 120, pp. 731–735, https://doi.org/10.1016/j.proeng.2015.08.776

33. Romero FJ et al (2019) Chemical design, fabrication and characterization of capacitive humidity sensors based on emerging flexible technologies. Sens Actuators B Chem 287(February):459–467. https://doi.org/10.1016/j.snb.2019.02.043

34. Rahman MT, Rahimi A, Gupta S, Panat R (2016) "Microscale additive manufacturing and modeling of interdigitated capacitive touch sensors," Sensors and Actuators A: Physical, vol. 248, pp. 94–103, https://doi.org/10.1016/j.sna.2016.07.014

35. Qin H, Dong J, Lee Y (2017) Fabrication and electrical characterization of multi-layer capacitive touch sensors on flexible substrates by additive e-jet printing. J Manuf Process 28:479–485. https://doi.org/10.1016/j.jmapro.2017.04.015

36. Jiang J, Ma Y (2020) Path planning strategies to optimize accuracy, quality, build time and material use in AM. Micromachines 11(7)

37. Jiang J, Xu X, Stringer J (2018) Support structures for additive manufacturing: a review. J Manuf Mater Process 2(4). https://doi.org/10.3390/jmmp2040064

38. Percoco G, Arleo L, Stano G, Bottiglione F (2021) Analytical model to predict the extrusion force as a function of the layer height, in extrusion based 3D printing. Addit Manuf 38(December 2020):101791. https://doi.org/10.1016/j.addma.2020.101791

39. Bellini A, Güçeri S, Bertoldi M (2004) Liquefier dynamics in fused deposition. J Manuf Sci Eng Trans ASME 126(2):237–246. https://doi.org/10.1115/1.1688377

40. Chen J, Smith DE (2021) Filament rheological characterization for fused filament fabrication additive manufacturing: a low-cost approach. Addit Manuf 47(March):102208. https://doi.org/10.1016/j.addma.2021.102208

41. Dey A, Yodo N (2019) A systematic survey of FDM process parameter optimization and their influence on part characteristics. J Manuf Mater Process 3(3):64. https://doi.org/10.3390/jmmp3030064

42. Helseth LE (2018) Nano energy interdigitated electrodes based on liquid metal encapsulated in elastomer as capacitive sensors and triboelectric nanogenerators. Nano Energy 50(April):266–272. https://doi.org/10.1016/j.nanoen.2018.05.047

43. Chetpattananondh K, Tapoanoi T, Phukpattaranont P, Jindapetch N (2014) Sensors and Actuators A : Physical A self-calibration water level measurement using an interdigital capacitive sensor. Sens Actuators A Phys 209:175–182. https://doi.org/10.1016/j.sna.2014.01.040

44. Ragolia MA, Lanzolla AML, Percoco G, Stano G, Di Nisio A (2021) Thermal characterization of new 3d-printed bendable, coplanar capacitive sensors. Sensors 21(19). https://doi.org/10.3390/s21196324

45. Schouten M, Wolterink G, Dijkshoorn A, Kosmas D, Stramigioli S, Krijnen G (2021) A review of extrusion-based 3D printing for the fabrication of electro- and biomechanical sensors. IEEE Sens J 21(11):12900–12912. https://doi.org/10.1109/JSEN.2020.3042436

46. Dijkshoorn A, Ravi V, Neuvel P, Stramigioli S, Krijnen G (2022) Mechanical interlocking for connecting electrical wires to flexible, FDM, 3D-printed conductors. FLEPS 2022 - IEEE Int Conf Flex Printable Sens Syst Proc 23–26. https://doi.org/10.1109/FLEPS53764.2022.9781552